Hou, Xuelan; Aitola, Kerttu; Lund, Peter D.

TiO_2 nanotubes for dye-sensitized solar cells—A review

Published in:
Energy Science and Engineering

DOI:
10.1002/ese3.831

Published: 29/10/2020

Document Version
Publisher's PDF, also known as Version of record

Received: 11 August 2020 | Revised: 17 September 2020 | Accepted: 24 September 2020

DOI: 10.1002/ese3.831

REVIEW

Energy Science & Engineering
Open Access

TiO_2 nanotubes for dye-sensitized solar cells—A review

Xuelan Hou | **Kerttu Aitola** | **Peter D. Lund**

New Energy Technologies Group, Department of Applied Physics, School of Science, Aalto University, Espoo, Finland

Correspondence
Xuelan Hou, New Energy Technologies Group, Department of Applied Physics, School of Science, Aalto University, Aalto, Espoo FI-00076, Finland.
Email: xuelan.hou@aalto.fi

Funding information
the Academy of Finland Flagship Programme, Photonics Research and Innovation (PREIN), Grant/Award Number: 320167; the Jane and Aatos Erkko Foundation ASPIRE project; China Scholarship Council, Grant/Award Number: 201706250038

Abstract

TiO_2 nanotubes (TNTs) are a potential candidate for the photoelectrode in dye-sensitized solar cells (DSSCs). In this review, emphasis is given to the fabrication methods of the TNT photoelectrode, including the anodic oxidation method, the hydro/solvothermal method, and the template method. Modification of TNTs to improve the power conversion efficiency (PCE) and the long-term stability of DSSCs is also covered. The active area of the DSSC strongly correlates with the PCE. Therefore, evaluating and comparing cell efficiencies with the same active area would be important. Reducing the material and manufacturing costs of TNT-based DSSCs will be an important future target.

KEYWORDS

active area, dye-sensitized solar cells, modification methods, scale effect, stability, TiO_2 nanotubes

1 | INTRODUCTION

Dye-sensitized solar cells (DSSCs) represent a relatively new potential photovoltaics technology due to the simple and low-cost processes for their manufacturing and wide range of applications.[1-3] The power conversion efficiency (PCE) and stability of DSSCs[4] have improved over time, the highest PCE now being 14.3%.[5] A typical DSSC is composed of a photoelectrode, a dye, an electrolyte, and a counter electrode (CE).[6] The PCE very much depends on the electron transfer "efficiency" at the different photoelectrode/dye/electrolyte/counter electrode interfaces[7] and the electron transport "efficiency" at the different cell components (PE, electrolyte, CE) as well as on the current collection ability of the photoelectrode. Therefore, the photoelectrode materials are important to the further development of the DSSCs,[1] in particular because of their importance to light absorption and electron transport.

Among the semiconducting photoelectrode materials, mesoporous TiO_2 is the most popular for DSSCs.[1,8] Often commercial TiO_2 nanoparticles (NPs) with a band gap of 3.0-3.2 eV[9] are employed as the photoelectrode, that offers fast electron transfer and a large number of contact sites to adsorb the dye molecules, that is, a high specific surface area.[10] However, grain boundaries may lead to electron recombination, which results in a photocurrent loss, and also to a loss of light absorption in the near-infrared region.[11] As an alternative to TiO_2 NPs, TiO_2 nanotubes (TNTs) have been considered as a promising photoelectrode option for DSSCs.[12,13] TNTs show improved light scattering, fast electron transport and low charge carrier recombination, and simple control geometry, compared with the NPs.[14,15] In addition, the tubular structure provides a relatively large contact surface area to decorate with metal oxide NPs and adsorb dye molecules on the photoelectrode.[16]

In 2002, Uchida et al[17] for the first time reported of a DSSC with TNTs as the photoelectrode (TNT length 100 nm, diameter 8-10 nm, active cell area 25 mm^2), which was produced by a hydrothermal method, showing an PCE of 2.9%. Later, anodic TNTs with a tube length of 500 nm and 2.5 μm were reported showing an PCE of 1.6% and 3.3%, respectively.[18] The highest

PCE reported is 10.2% with nanotwinned TNTs in DSSC using N719 dye with an active area of 20 mm^2.[19] This value is still lower than that of a TiO_2 NP-based DSSC (14.7%).[5]

The literature on using TiO_2 TNTs in DSSCs is still limited albeit the potential of this technology.[20,21] Here, we will present a state-of-the art of this technology. The focus is on the preparation methods of TNTs for DSSC and on the modification methods of TNTs to improve the PCE of DSSCs. Key parameter values and critical factors limiting the performance of TNTs are summarized. The stability issues of TNT-based DSSCs are also briefly discussed, an important topic for DSSCs in general. Finally, possible future research areas for promoting the development of TNT-based DSSCs will be proposed.

2 | PRINCIPLE AND STRUCTURE OF DYE-SENSITIZED SOLAR CELL

The structure and operational principle of DSSCs are shown in Figure 1.[6,22] A typical DSSC is composed of a photoelectrode (typically around 10 μm thick mesoporous TiO_2 film comprising of around 20 nm nanoparticles, on a transparent conducting oxide-coated glass, TCO glass, substrate), a dye (eg, ruthenium metal complex dye "N719" or an organic dye), electrolyte (eg, I^-/I_3^- redox couple in an organic solvent), and counter electrode (typically platinum on TCO glass).[6] In a DSSC, the dye absorbs photons from incident solar light to generate electrons.[6] The photons need to match the energy level difference of the dye. From the excited energy level of the dye, the electrons are injected into the conduction band (CB) of the TiO_2. Then, the electrons diffuse through the TiO_2 and are transported to an external electrical circuit to provide electrical current. The oxidized dye is reduced by the electrolyte redox mediator ion (such as I^-, or Co^{2+} metal complex ion). The platinum CE collects the electrons from the external circuit and reduces the oxidized electrolyte redox mediator, thus closing the electrical circuit.[22]

The performance of a DSSC is described by the power conversion efficiency. The PCE of the cell depends on the short-circuit current (J_{sc}, mA/cm^2), the open circuit voltage (V_{oc}, V), fill factor (FF), and the incident sunlight (P_{in}, normally 100 mW/cm^2, AM 1.5G spectrum) on the cell.[22] The PCE can be written as:

$$\mathrm{PCE} = \frac{V_{oc} J_{sc} \mathrm{FF}}{P_{in}} \times 100\%, \tag{1}$$

where the fill factor is defined as

$$\mathrm{FF} = \frac{V_{mpp} J_{mpp}}{V_{oc} J_{sc}}, \tag{2}$$

V_{mpp} and J_{mpp} correspond to the voltage and current values at the maximum power point (MPP).

3 | PREPARATION METHODS OF TNTS FOR DSSC

There are many methods to prepare TNTs, such as the anodic oxidation method,[23-30] the hydro/solvothermal synthesis method,[31-37] and the template method.[7,11-15] In the following, the preparation methods of TNTs for DSSCs are explained in more detail.

3.1 | Anodic oxidation method

Most publications have reported fabricating TNTs by the anodic oxidation method, and there are 12 328 publications on the topic in the Web of Science Core Collection (keywords: TiO_2 nanotubes, and anodic oxidation, or anodization, time span:1945-2020).

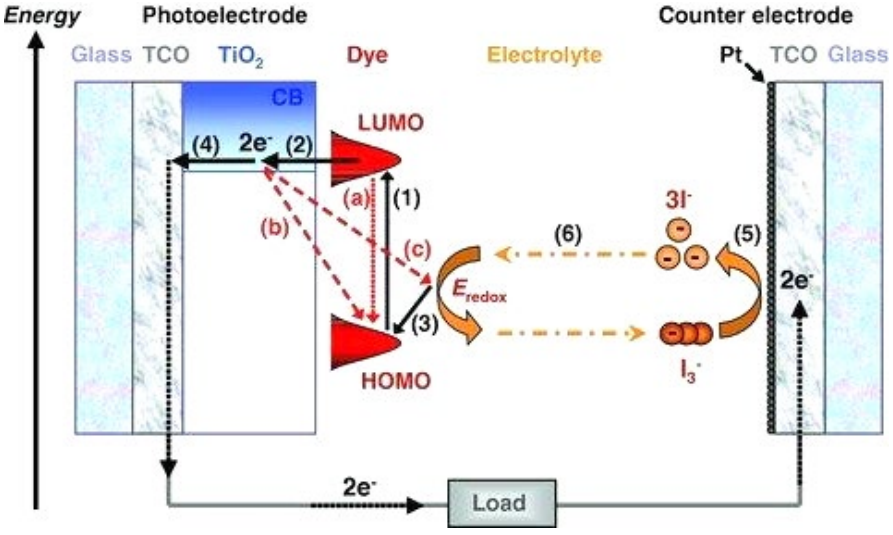

FIGURE 1 The structure, energy levels, and the operating principle of a typical dye-sensitized solar cell,[6] reproduced from reference 6 with permission from WILEY-VCH Verlag GmbH & Co. KGaA, Weinheim, 2010

The anodic oxidation method of the TNT preparation is carried out with a DC power supply at a constant voltage or current in a two-electrode system, where titanium (Ti) metal functions as the working electrode and typically Pt as the counter electrode. The setup is shown in Figure 2. It is worthwhile to mention that the Ti metal is cheaper than FTO glass, also having good flexibility, and a low sheet resistance, and it would be suitable for high temperature treatment.[38-41]

Yun et al[16] adopted the anodic oxidation method to prepare the photoelectrode TNTs/Ti at a constant voltage of 60 V in an electrolyte consisting of ethylene glycol (EG) containing 0.5 wt. % NaF and 5 wt. % H_2O. They varied the reaction time (1, 5 and 15 hours) to produce TNTs with the lengths of 3, 10, and 22 μm, yielding PCEs of 0.55%, 1.45%, and 1.88%, respectively, under a 60 minutes 1 sunlight soaking treatment. Luo et al[24] prepared vertically oriented TNTs on a Ti mesh by the anodic oxidation method at an constant voltage of 30 V with reaction times of 10-30 hours to adjust the tube length from 9 μm to near 20 μm. It showed the highest PCE of 2.66% when the tube length is ~18 μm. Yi et al[23] investigated the effects of the electrolyte water content and the anodizing time on the TNT-based DSSCs. It was found that when the water content was 2 vol %, the cells showed the best performance, due to the increased TNT diameter resulting in increased specific surface area of the tube surface and dye loading ability. In order to match the energy levels with the N719 dye, Xie et al[4] prepared the TiO_2 nanotube photonic crystals (NTPCs) with a ~150 nm lattice by a two stage anodic oxidation method. The first step was the anodic oxidation method, and in the second step, they adopted a high periodic alternating current (anodic voltage ~60 V, time 30 seconds) and low current (0 A, 90 seconds) pulses to prepare the NTPCs by controlling the pulse number (N = 15, 30, 45 and 60) to obtain lattices with different thicknesses, and the details and results showed in Table 1, N = 5. Ji et al[25] realized bamboo-type double-walled TNTs (DBN) on Ti metal substrates. The benefit of the structure was improved dye loading and PCE. The dye loading of DBN-1 (double-walled, bamboo-type nanotubes, grown under AV conditions, with a sequence of 2 minutes at 120 V and 12 minutes at 40 V for 8 hours anodization) and DBN-2 (double-walled bamboo-type tubes, grown under AV conditions, with a sequence of 4 minutes at 120 V and 12 minutes at 40 V for 6 hours anodization) was 3.2×10^{-8} mol/cm^2 and 2.4×10^{-8} mol/cm^2, which was higher than the dye adsorption ability of smooth-walled TNTs (1.9×10^{-8} mol/cm^2).

Employing the anodic oxidation method to prepare TNTs directly on Ti metal is appealing not only because Ti is an ideal candidate for a DSSC substrate due to its high bending ability under external force,[24] but also because the resulting TNTs are aligned in a highly ordered manner. They have a high length-to-diameter ratio (Figure 3) and excellent electron transporting performance, they can be fabricated conformally over large areas, the Ti metal and TNTs/Ti acts as an electrode in electrochemical devices, and they are feasible for several practical applications.[24,42-54] Some publications reported sputtered Ti metal (sputtered Ti thickness 1-2 μm) on transparent conductive oxide (TCO) glass substrate to prepare TNTs by the anodic oxidation method,[55-57] to avoid the losses caused by the necessarily employed back illumination decreasing the light-harvesting capability, when the TNTs are prepared on the opaque Ti metal.

3.2 | Hydro/solvothermal method

The hydrothermal method is an effective and cost-effective way to prepare TNTs,[31-37] and there are 3903 publications on the topic in the Web of Science Core Collection (keywords: TiO_2 nanotubes, hydrothermal, solvothermal, time span:1945-2020).

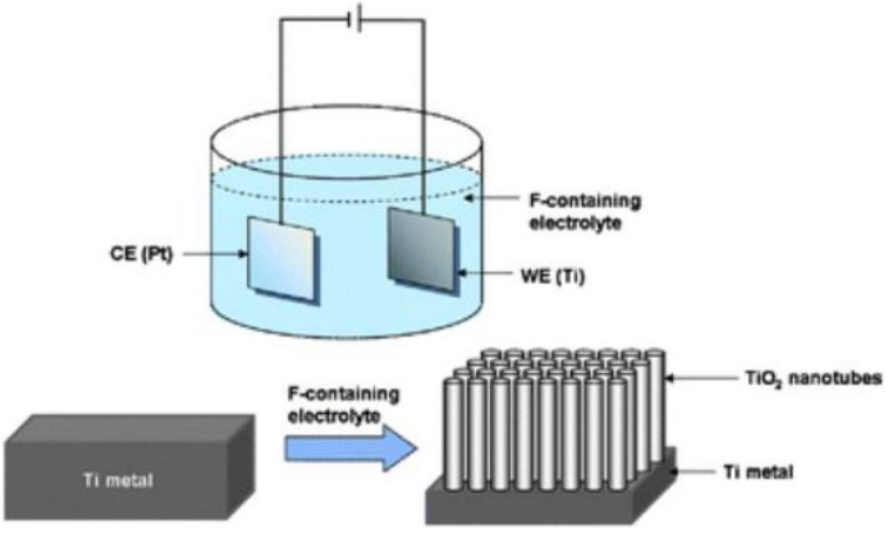

FIGURE 2 A schematic diagram of a electrochemical set-up and the anodic growth of TiO_2 nanotubes on a Ti metal sheet,[20] reproduced from reference 20 with permission from Copyright of Royal Society of Chemistry (Great Britain), 2010

TABLE 1 Summary of TiO_2 nanotubes-based photoanode in DSSCs, preparation methods, cell size, dye, counter electrode, electrolyte, and corresponding photovoltaic parameters, under simulated AM-1.5 illumination (power 100 mW/cm^2)

Number	Methods	Cell size (mm^2)	Parameters of TNTs Length = L (μm) Pore diameter = D (nm)		Dye	CE
1	Anodic oxidation	36	$L = 3.32 \pm 0.06$ $D = 50.01 \pm 2.35$ $L = 10.45 \pm 0.53$ $D = 78.61 \pm 5.55$ $L = 22.32 \pm 0.85$ $D = 98.67 \pm 4.87$		Porphyrin (GD2)	Pt/FTO
2	Anodic oxidation	100	$L = 14.3$ $L = 17.3$ $L = 18.3$ $L = 19.2$		N719	SputteredPt/Ti foil
3	Anodic oxidation	49	$L = 5$ $L = 10$ $L = 15$ $L = 20$		N719	Coated Pt/FTO
4	Anodic oxidation	16	$L = 15$ $D = 100$ $L = 22$ $D = 100$ $L = 35$ $D = 100$ $L = 30$ $D = 100$ $L = 30$ $D = 100$		0.3 mmol/L N719	Coated Pt/FTO
5	Anodic oxidation	16	10 μm NP 10 μm NP +15c NTPC ~10 μm NP +30c NTPC ~10 μm NP +45c NTPC ~10 μm NP +60c NTPC	 $L = 2.3$ $L = 4.5$ $L = 6.7$ $L = 9$	0.3 mmol/L N719	Coated Pt/FTO
6	Anodic oxidation	20	Cylinder NT (Notreatment) 2 times $TiCl_4$ -Cylinder NT Cone NT (Notreatment) 5 times $TiCl_4$ -Cone NT	$L = 13$	0.3 mmol/L N719	Coated Pt/FTO
7	Anodic oxidation	20	NT NT + NP NT + NP + SiO_2 NT + NP + Al_2O_3	$L = 12$ $D > 500$	0.3 mmol/L N719	Coated Pt/FTO

Electrolyte	J_{sc} (mA/cm^2)	V_{oc} (V)	FF	PCE (%)	Ref.
A mixture of 0.1 mol/L LiI, 0.6 mol/L 1, 2dimethyl-3propylimidazoliumiodide (DMPII), 0.03 mol/L I_2, and 0.5 mol/L t-butylpyridine (TBP) in acetonitrile	1.36	0.49	0.56	0.37	16
	2.33	0.48	0.53	0.59	
	2.69	0.48	0.66	0.70	
A mixture of 0.1 mol/L LiI, 0.6 mol/L DMPII, 0.05 mol/L I_2, and 0.5 mol/L TBP in acetonitrile	4.3	0.7	0.62-0.66	2.04	24
	x	x		2.27	
	x	x		2.32	
	6.5	0.67		2.30	
A mixture of 0.3 mol/L LiI, 0.6 mol/L DMPII, 0.03 mol/L I_2, 0.1 mol/L GuNCS, and 0.5 mol/L TBP in acetonitrile	2.02	0.6	0.42	0.50	23
	3.02	0.69	0.49	1.03	
	3.95	0.71	0.55	1.54	
	5.2	0.70	0.54	1.96	
A mixture of 0.1 mol/L LiI, 0.6 mol/L DMPII, 0.01 mol/L I_2, 0.1 mol/L GuNCS, and 0.5 mol/L TBP in acetonitrile	10.26	0.790	0.723	5.9	119
	11.68	0.783	0.701	6.4	
	13.12	0.762	0.661	6.6	
	12.84	0.779	0.703	7.0	
0 wt % PMMA-EA	12.95	0.771	0.707	7.1	
4 wt % PMMA-EA	11.82	0.782	0.687	6.4	
7 wt % PMMA-EA	12.68	0.791	0.684	6.9	
10 wt % PMMA-EA	12.05	0.786	0.655	6.2	
13 wt % PMMA-EA	11.08	0.766	0.649	5.5	
A mixture of 0.1 mol/L LiI, 1.0 mol/L DMPD, 0.12 mol/L I_2, 0.5 mol/L TBP, and 3-methoxy propionitrile (purchased electrolyte)	11.09	0.706	0.598	4.68	4
	15.57	0.705	0.618	6.78	
	16.10	0.706	0.625	7.1	
	14.69	0.697	0.604	6.19	
	13.22	0.693	0.613	5.62	
A mixture of 0.60 mol/L BMIM-I, 0.03 mol/L I_2, and 0.10 mol/L GTC in acetonitrile and valeronitrile (85:15 vol.) (purchased electrolyte)	10.18	0.76	0.553	4.28	93
	13.31	0.76	0.493	5.04	
	6.69	0.84	0.560	3.15	
	15.63	0.79	0.655	8.09	
A mixture of 0.60 mol/L BMIM-I, 0.03 mol/L I2, and 0.10 mol/L GTC in acetonitrile and valeronitrile (85:15 vol.) (purchased electrolyte)	7.50	0.710	0.52	2.78	89
	12.90	0.754	0.60	5.84	
	14.70	0.754	0.61	6.71	
	14.35	0.754	0.59	6.35	

(Continues)

Number	Methods	Cell size (mm^2)	Parameters of TNTs Length = L (μm) Pore diameter = D (nm)		Dye	CE
8	Anodic oxidation	50	SNT	$L = 10$ $D = 100$	0.3 mmol/L N719	Coated Pt/FTO
			DBN-1	$L = 10$ Inner $d = 70$ $D = 230$		
9	Anodic oxidation	12	S	$L \approx 10.5$	0.2 mmol/L N719	Coated Pt/FTO
			S-H			
			S-T			
			S-H-O_2			
10	Anodic oxidation	x	Reference NT	$L = 15$ $D = 120$	0.3 mmol/L N719	x
			Ta 0.03 at%			
			Ta 0.1 at%			
			Ta 0.4 at%			
11	Anodic oxidation	20	Air-450		0.3 mmol/L N719	Coated Pt/FTO
			Air-550			
			Air-650			
			Air-750			
			O_2-450			
			O_2-550			
			O_2-650			
			O_2-750			
			1$TiCl_4$-O_2-650			
			2$TiCl_4$-O_2-650			
			3$TiCl_4$-O_2-650			
12	Anodic oxidation	16	TNTA/FTO	$D = 126$	0.5 mmol/L N719	Sputtered Pt/FTO
			Au-TNTA	$D \sim 126$		
			MH-TNTA-3	$L = 15.2$ $D = 66$		
			H-TNTA-3	$L = 15.2$ $D = 66$		
			MH-TNTA-3 ($TiCl_4$treatmen)	$D \sim 66$		
13	Anodic oxidation	x	TNT-DSSC	$L = 33$ $D = 120$	0.3 mmol/L N719	Sputtered Pt/FTO
			$TiCl_4$-DSSC	$L = 33$ $D \sim 100$		
			TNT-TNA-DSSC	$L = 33$ $D \sim 60$		
14	Anodic oxidation	x	Untreated	$L = 19.3$ $D = 120$	0.3 mmol/L N719	Sputtered Pt/FTO
			0.025 mol/L HCl			
			0.05 mol/L HCl			
			0.1 mol/L HCl			
			0.1 mol/L HCl			

Electrolyte	J_{sc} (mA/cm^2)	V_{oc} (V)	FF	PCE (%)	Ref.
A mixture of 0.1 mol/L LiI, 0.05 mol/L I_2, and 0.5 mol/L TBP in acetonitrile	5.4	0.68	0.57	2.01	25
	7.4	0.72	0.63	3.46	
A mixture of 0.60 mol/L BMIM-I, 0.03 mol/L I_2, 0.10 mol/L GTC, and 0.50 mol/L TBP in acetonitrile and valeronitrile (85:15 vol.)	11.74	0.72	0.51	4.3	94
	14.31	0.79	0.63	7.12	
	12.77	0.77	0.67	6.54	
	15.64	0.77	0.62	7.75	
x	11.03	0.76	0.484	4.06	98
	14.62	0.70	0.401	4.44	
	14.87	0.72	0.475	5.09	
	15.68	0.71	0.438	4.88	
A mixture of 0.60 mol/L BMIM-I, 0.03 mol/L I_2, and 0.10 mol/L GTC in acetonitrile and valeronitrile (85:15 vol.) (purchased electrolyte)	15.42	0.78	0.6306	7.58	19
	15.88	0.8	0.6344	8.06	
	16.77	0.82	0.6297	8.66	
	17.04	0.78	0.6199	8.24	
	15.83	0.79	0.6285	7.86	
	16.25	0.834	0.6220	8.48	
	17.10	0.883	0.6225	9.4	
	17.33	0.864	0.6112	9.15	
	17.34	0.897	0.6382	9.94	
	17.71	0.891	0.6483	10.23	
	18.08	0.873	0.6076	9.59	
A mixture of 0.5 mol/L LiI, 0.3 mol/L HMII, 0.05 mol/L I_2, 0.3 mol/L NMB, and 0.5 MTBP in 3-ethoxypropionitrile	10.15	0.745	0.62	4.69	86
	10.86	0.722	0.66	5.18	
	16.25	0.765	0.69	8.54	
	15.31	0.771	0.67	7.91	
	16.85	0.785	0.68	8.93	
A mixture of 0.60 mol/L BMII, 0.03 mol/L I_2, 0.10 mol/L CuSCN, and 0.5 mol/L TBP in acetonitrile and valeronitrile	12.27	0.62	0.6301	4.76	85
	21.50	0.66	0.6237	8.90	
	24.78	0.71	0.5596	9.86	
A mixture of 0.60 mol/L BMII, 0.03 mol/L I_2, 0.10 mol/L CuSCN, and 0.5 mol/L TBP in acetonitrile and valeronitrile	11.56	0.707	0.6042	4.94	116
	12.80	0.739	0.6400	6.05	
	14.12	0.735	0.6334	6.57	
	16.81	0.728	0.6896	8.44	
	15.21	0.724	0.6184	6.81	

(Continues)

Number	Methods	Cell size (mm^2)	Parameters of TNTs Length = L (μm) Pore diameter = D (nm)		Dye	CE
15	Anodic oxidation	260-300	TNT	$L = 33$	0.3 mmol/L N719	Sputtered Pt/FTO
		13	TNT	$L = 33$		
			TNT-$TiCl_4$ treatment	$L = 33$		
16	Anodic oxidation	25	NPs coated on TNTs/Ti	$L \sim 5$ $D \sim 150$	0.3 mmol/L N719	Coated Pt/FTO
		100				
		400				
		900				
		25	NPs/FTO			
		100				
		400				
		900				
17	Hydrothermal	20	P25		0.5 mmol/L N719	Pt/FTO
			P25 + G2			
			P25 + C-TNT			
			P25 + C-TNT Comp.			
			P25 + HF-TNT			
			P25 + HF-TNT Comp.			
18	Hydrothermal	28.3	T0P1		0.3 mmol/L N719	Sputtered Pt/FTO
			T0.1P1			
			T1P1			
			T3P1			
			T10P1			
			T10P1			
19	Hydrothermal	14-18	TiO_2 NPs		0.3 mmol/L N3	Coated Pt/FTO
			Nb-doped TiO_2 NPs			
			TiO_2 NTs			
			Nb-doped TiO_2 NTs			
20	ZnO template	36	TiO_2 90 min	x	0.5 mmol/L N719	Coated Pt/FTO
			TiO_2 1.5 h	$L = 1.6 \pm 0.1$ $D_o = 87 \pm 9$ $D_i = 50 \pm 6$		
			TiO_2 4.5 h	$L = 1.7 \pm 0.1$ $D_o = 130 \pm 10$ $D_i = 40 \pm 5$		
			TiO_2 6 h	$L = 1.8 \pm 0.1$ $D_o = 200 \pm 12$ $D_i = 40 \pm 5$		
			TiO_2 15 h	$L = 2.7 \pm 0.4$ $D_o = 850 \pm 20$ $D_i = 235 \pm 15$		
21	ZnO template	25	TNT	$L = 20$	0.5 mmol/L N719	sputtered Pt/FTO
22	AAO template ALD	x	CE-DSSC closed	$L = 8$ $D = 70$	0.5 mmol/L N719	FTO
			OE-DSSC open			

Note: x: the data are not shown in the related publications.

Electrolyte	J_{sc} (mA/cm^2)	V_{oc} (V)	FF	PCE (%)	Ref.
A mixture of 0.60 mol/L BMII, 0.03 mol/L I_2, 0.10 mol/L CuSCN, and 0.5 mol/L TBP in acetonitrile and valeronitrile	12.39	0.62	0.545	4.12	71
	11.47	0.63	0.668	4.86	
	22.76	0.65	0.614	9.02	
A mixture of 0.60 mol/L BMII, 0.03 mol/L I_2, 0.10 mol/L GTC, and 0.5 mol/L TBP in acetonitrile and valeronitrile (85:15 vol.)	9.36	0.79	0.66	4.82	13
	9.69	0.75	0.61	4.50	
	9.68	0.73	0.61	4.35	
	9.72	0.67	0.45	2.92	
	17.90	0.81	0.55	7.92	
	14.70	0.82	0.54	6.56	
	13.20	0.80	0.28	2.96	
	5.99	0.77	0.25	1.18	
A mixture of 0.1 mol/L LiI, 0.6 mol/L PMII, 0.05 mol/L I_2, and 0.5 mol/L TBP in a mixture of acetonitrile and valeronitrile (85:15 vol.)	13.715	0.758	0.74	7.7	31
	15.925	0.752	0.75	9.036	
	15.709	0.741	0.759	8.856	
	16.319	0.737	0.764	9.201	
	17.275	0.738	0.764	9.743	
	18.135	0.732	0.766	10.168	
Oligo-PEGDME electrolyte	6.93	0.60	0.48	1.99	60
	7.80	0.59	0.46	2.14	
	2.97	0.58	0.57	0.96	
	0.60	0.6	0.59	0.21	
	0.2	0.56	0.52	0.06	
DMPII ionic liquid electrolyte	20.72	0.7	0.71	10.27	
Commercially electrolyte AN-50 (Solaronix)	Best cell				7
	14.0	0.70	0.61	6.0	
	14.3	0.68	0.67	6.5	
	14.6	0.73	0.66	7.1	
	15.0	0.72	0.75	8.1	
A mixture of 0.1 mol/L LiI, 0.60 mol/L DMPII, 0.05 mol/L I_2, 0.10 mol/L GTC, and 0.5 mol/L TBP in acetonitrile and valeronitrile (85:15 vol.)	0.76	0.76	0.65	0.37	65
	1.41	0.77	0.67	0.73	
	2.47	0.75	0.59	1.10	
	3.42	0.76	0.68	1.77	
	5.06	0.76	0.64	2.46	
A mixture of 0.60 mol/L BMII, 0.03 mol/L I_2, 0.10 mol/L CuSCN, and 0.5 mol/L TBP in acetonitrile and valeronitrile	7.0	0.84	0.75	4.4	64
A mixture of 0.60 mol/L BMII, 0.03 mol/L I_2, 0.10 mol/L GTC, and 0.5 mol/L TBP in acetonitrile and valeronitrile (85:15 vol.)	2.32	0.71	0.38	0.63	67
	3.81	0.75	0.43	1.17	

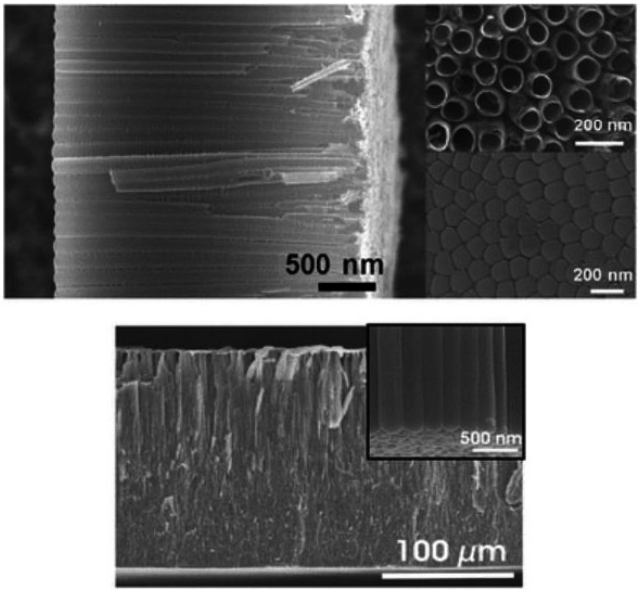

FIGURE 3 SEM images of TiO_2 nanotube layers formed by the anodic oxidation of Ti- metal (cross section, top view and bottom view),[20] reproduced from reference 20 with permission from Copyright of Royal Society of Chemistry (Great Britain), 2010

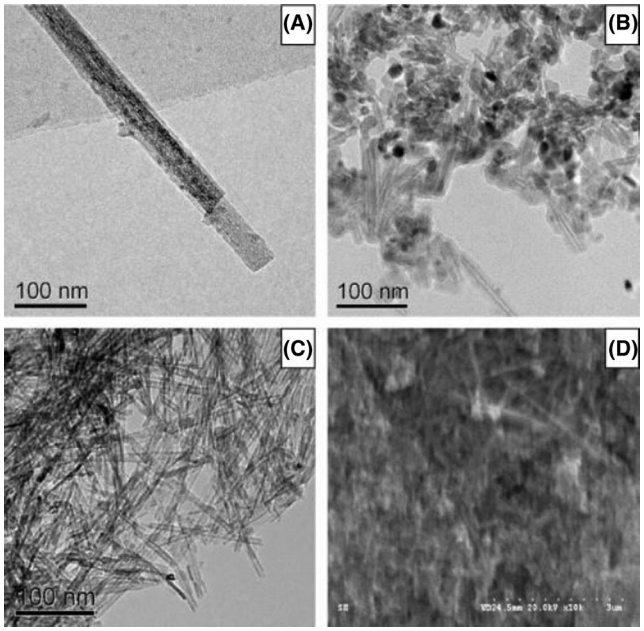

FIGURE 4 TEM images of (A) TNT-A, (B) TNT-B, (C) TNT-C, and (D) SEM image of TNT-C and P25,[34] reproduced from reference 34 with permission from Copyright © 2010 Elsevier Ltd

The typical hydrothermal method to prepare TNTs consists of mixing commercial P25 TiO_2 powder and an aqueous NaOH solution together in a Teflon autoclave at a temperature of 100-150°C,[58] which is also suitable for the preparation of TNTs/TiO_2 NP composites used for DSSC photoelectrode fabrication (SEM is shown in Fig. 4).[34,59-62]

Qadir et al[31] prepared highly functional TNTs by a hydrothermal method, which showed 68% higher dye loading ability than conventional TNTs and also 50% higher photocatalytic degradation rate. The PCE of the highly functional TNT-based DSSCs was 10.1%. First, a solution was prepared with 12 mol/L NaOH aqueous solution [160 mL, in deionized water (DI) water] and 3 g of new precursor SG-T0200 TiO_2 nanoparticles with magnetic stirring for 1 hour. SG-T0200 particles (Sukgyung AT) are much larger than the conventional precursor nanoparticles (P25), resulted in a 68% enhancement of dye loading. After 15 minutes of ultrasonication, the solution was heated at 130°C with stirring for 48 hours. When the solution was cooled down to room temperature, 0.05 mol/L HCl (aq.) was added to maintain its pH at 1.0. After a DI water washing and a centrifugation process, the prepared slurry was placed in the hydrothermal instrument again, with another heating and stirring process at 200°C for 12 hours. In the end, it was annealed at 430°C for 4 hours to obtain the anatase TNTs. Tsvetkov et al[7] reported Nb-doped TNTs by using Nb-doped TiO_2 NPs as a starting material, which were first dissolved in 100 mL of 10 mol/L NaOH aqueous solution and autoclaved for 12 hours at 120°C. Then, 150 mL of 0.1 mol/L HCl (aq.) was added in the solution, followed by centrifugation in water and ethanol to obtain Nb-doped TNTs. The ratio of TNTs and TiO_2 NPs can affect the charge transfer and electron lifetime, further impacting the PCE in DSSCs[60] (Table 1, number 18). In order to prepare well-aligned hierarchical TiO_2 nanotubes (HTNTs) in a simple and cost-effective way, Chen et al[32] adopted a one-step hydrothermal method with potassium titanium oxalate, ethanol and H_2O. In the beginning, TiO_2 collosol was spin coated on fluorine-doped tin oxide (FTO) glass substrate to form a seed layer. After mixing potassium titanium oxalate, ethanol, and H_2O in a Teflon liner and stirring for 1 hour, an FTO glass with the seed layer was immersed in the solution and heated in the oven at 200°C with varying times of 3, 6, 9, 12, and 15 hours to produce hierarchical TNTs with the tube lengths of 12, 16, 18, 20, and 22 μm, the corresponding PCE of the cell were 3.43%,7.45%, 9.30%, 9.89%, and 8.36%. Not only well-aligned hierarchical TNTs applied in the assemble of DSSCs, but also pine tree-like TNTs were synthesized by a similar one-step hydrothermal method in a Teflon-lined stainless steel autoclave with the chemicals of PTO, water, and diethylene glycol at 200°C for 11 hours.[32,63] The pine tree-like TNTs give a potential to improve the adsorption ability of dye on the photoelectrode to enhance the PCE of DSSCs.

3.3 | Template-assisted method

There are 1350 publications on the topic of template method to prepare TNT in the Web of Science Core

Collection (keywords: TiO_2 nanotubes and template, time span:1945-2020).

Using ZnO nanowires as a template to prepare TNTs is a common method to manufacture TNT-based DSSCs.[64-66] It is carried out by immersing a ZnO nanowire template in a TiO_2 sol, ethanol and water for 30 seconds and repeating the procedure 20 times to form a TiO_2 shell with a thickness of 20-40 nm on the ZnO nanowires. Next, the obtained core/shell structure is annealed immediately at 350°C, followed by an etching process with 10 mmol/L $TiCl_4$ solution at room temperature, for the transformation of the core/shell structure into TNTs (Fig. 5).[64] Also Zhang et al[65] reported a template method to prepare TNTs by immersing a ZnO nanowire template in an aqueous solution of 0.075 mol/L $(NH_4)_2TiF_6$ and 0.2 mol/L H_3BO_3 at room temperature for 90 minutes to 15 hours. Lee et al[67] employed anodic aluminum oxide (AAO) as a template for an atomic layer deposition technique to fabricate open-end and close-end TNTs. Using titanium tetraisopropoxide ($Ti[OCH(CH_3)_2]_4$) and water as precursors to produce the TiO_2-deposited AAO, the sample was annealed at 450°C for 3 hours to form the anatase crystal structure. After removing the AAO template, crystalline anatase TNTs were obtained.

3.4 | Summary of performance of TNT photoelectrodes in DSSCs

A summary of TNT-based DSSCs using different manufacturing methods is given in Table 1 with key parameters shown. A detailed analysis of the TNT photoelectrode is given in the following Section.

4 | MODIFICATION OF TNT PHOTOELECTRODE TO IMPROVE THE EFFICIENCY OF DSSC

The specific surface area of TNTs is lower than that of the conventional TiO_2 NPs, which limits the amount of the adsorbed dye molecules on the photoelectrodes and therefore decreases the solar cells' light-harvesting efficiency. Thus, many modification methods have been investigated to minimize the aforementioned issues in TNTs in order to enhance the overall power conversion efficiency of TNT-based DSSCs.[1,68] Some results of the modifications of TNTs to fabricate DSSCs are summarized in Table 1. A lot of work has also been carried out to tune the energetic band levels of TNTs to better match those of the dyes[58] and to enhance the electron transfer in TNTs.[16] The most reported modification methods are explained in the following.

4.1 | Geometry of the TNTs and the resulting films

Larger surface area of the TNT films can be obtained by increasing the tube length and tuning the pore size of the tubes. With increasing the tube length, the electron lifetime and the diffusion length can be increased, followed by a significantly increased photocurrent density (J_{sc}).[16,24,38,66,69-76] 3, 10, and 22 μm long TNTs yielded solar cell PCEs of 0.37%, 0.59%, and 0.70%, respectively.[16] Joseph et al[77] found out that the counter electrode material in the electrochemical preparation of TNTs has an effect on the tube length and also the PCE in DSSCs. Platinum, titanium, iron, graphite pencil, and charcoal rod CEs yielded TNT lengths of 102,

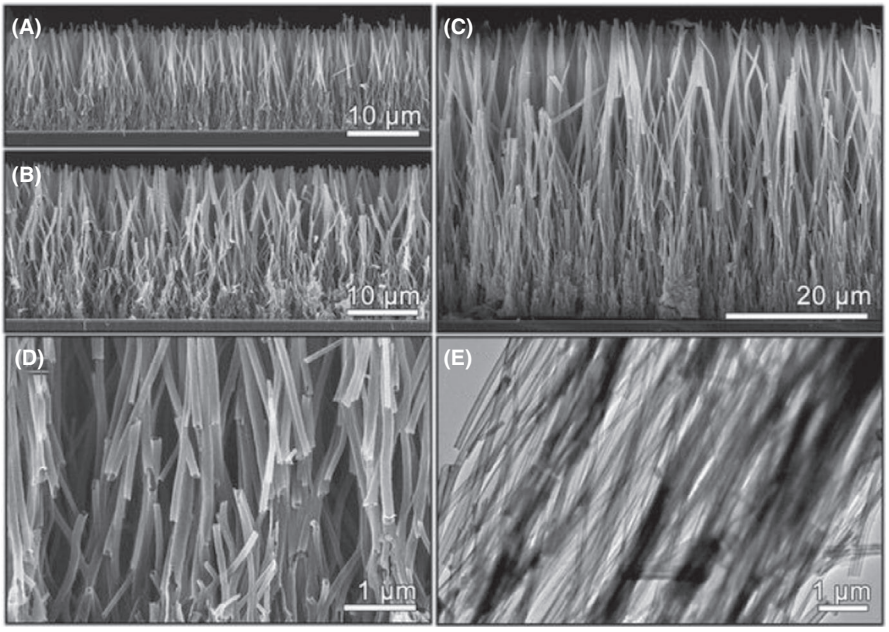

FIGURE 5 A cross section SEM images of TiO_2 nanotube arrays with various thicknesses: A, 13 μm, B, 20 μm, and C, 41 μm. D, E, Magnified SEM and TEM images revealing the well-defined nanotube structures.[64] Reproduced from reference 64 with permission from WILEY-VCH Verlag GmbH & Co. KGaA, Weinheim, 2011

130, 38, 55, and 88 μm, respectively, with a 24 hours anodization. Nyein et al[78] prepared TNTs in the electrolyte of KOH/fluoride/EG, LiOH/fluoride/EG, and H_2O/fluoride/EG at 60 V for 1 hour with the DC device and obtained TNTs with lengths of 18, 15, and 10 μm, respectively, and the corresponding PCEs in DSSCs were 3.0%, 2.7%, and 1.3%. The pore size of the TNTs can affect the dye loading and the light absorption ability. Qadir et al[31] prepared highly functional TNTs, with large pore diameters, resulting in a 68% improved dye loading and enhanced light absorption. Xie et al[4,79,80] adopted a periodic alternating high current and low current pulses to prepare TiO_2 NTPCs with a ~150 nm lattice constant, which had well matched band gap with the light absorption range of N719 dye under AM 1.5G.

4.2 | Decorating TNTs with nanoparticles

Decorating the TNTs with nanoparticles (NPs) is a common modification method to increase the active area of TNTs to improve the PCE of TNT-based DSSCs,[81] which is due to the enhanced dye absorption ability and promoted charge transfer.[67,82,83] TiO_2 NPs are the most used NPs to enhance the PCE in DSSCs.[70,81,84-87] Zhang et al[85] employed a sol-gel method to introduce TiO_2 NPs to decorate TNTs, which yielded the highest DSSC PCE of 9.86% (pristine TNT-DSSC, PCE = 4.76%) due to the increased specific surface are for enhanced dye absorption.

Depositing a thin layer of Al_2O_3[88,89] or SiO_2[89] on the surface of TNTs improved the PCE too, because the recombination rate of the charge carriers was reduced. ZnO[90-92] layer was utilized to decorate the TNTs to enhance the DSSC performance, resulting in lower recombination rate and charge transfer resistance.

4.3 | $TiCl_4$ treatment

The $TiCl_4$ treatment is not only a common modification method of TiO_2 NP-based in DSSCs, but also one of the most used modification methods to increase the specific surface area and improve the electron collection efficiency of TNT films in DSSCs. Schmuki's group[2,89,93] as well as other groups[43,44,64,71,72,84,86,88,94-97] modified TNTs with the $TiCl_4$ treatment (different times $TiCl_4$ treatment) to improve the electron collection and increase the surface area for enhancing the dye loading ability. The $TiCl_4$ treatment lead a back-side illuminated TNT-based DSSCs to yield a considerable PCE close to 8%, due to resulted in a multiple layered decoration to give a further improvement of the electronic properties.[2]

4.4 | Doping

Doping is a mature and effective way to modify the electronic structure of TNTs. Ta-doped TNTs layers were prepared on TiTa alloy foils (Ta 0.03 at. %, 0.1 at. %, and 0.4 at. %) = by the anodic oxidation method. The PCE of DSSCs with Ta-doped TNTs was improved by 9.77%, 124.8%, and 121.1% when compared with pure TNTs.[98] Also C,[99] N,[100] Cr,[58] Cu,[3] Nb,[7] and Li[101] doping of NTs to fabricate DSSCs has been investigated with PCEs of 6.59%, 7.91%, 8.69% (Cr/Ti atomic percentage is 7.50%), 0.30% (5.2% Cu doped), 8.1%, and 6.4% ($c(Li^+)$ = 50 mmol/L). Introducing noble metal Au[86,102,103] and Ag NPs[83,87,104-107] into TNTs can improve the PCE of the DSSCs, due to the enhanced light harvesting via surface plasmon resonance. The electrophoretic deposition technology was applied to deposit reduced graphene oxide,[108] TiO_2 NPs,[96,109] Au NPs,[99,102] and Ag NPs[105] to modify TNTs to enhance the PCE of DSSCs. Both a hydrothermal process and an O_2 plasma exposure improved the dye absorption on the TNT photoelectrode[94] by creating rough surfaces and hydroxyl groups on the TiO_2. Fu et al[86] prepared multi-hierarchical TNTs by introducing Au clusters on the walls of the TNTs by the photoreduction approach and filling TiO_2 NPs into TNTs, yielding a PCE of 8.93%, which is 190.4% better than that of the pristine TNT-based DSSCs. The Au NPs directly injected hot electrons into the semiconductor to accelerate electron transfer and improve the light harvesting in the DSSCs.[79]

4.5 | Open-end TNTs

Open-end TNT-based DSSCs are often reported to have a higher PCE than closed-end TNT-based DSSCs.[67,110,111] Lin et al[112] obtained a DSSC PCE of 9.1% with open-end TNTs, which was explained by an enhanced light harvesting and electron collection ability due to the open-end TNTs helping the redox electrolyte easily reaching the NP-TiO_2 underlayer, which was printed on the FTO to fabricated the open-end TNT-based DSSC. Zhu et al[44] employed abrasive paper (3000 mesh) to abrade the fixed membrane or adopted manual grinding polisher (~100 rpm) to remove the closed bottom caps of anodic TNTs to achieve open-end TNTs, which resulted in a DSSC PCE of 7.7%, a 66% enhancement compared with the pristine TNTs based DSSCs.

4.6 | Annealing conditions

The annealing temperature[19,100-101,113-115] and atmosphere[19] affect the crystallization of the TNTs, further impacting the electron transport in the resulting films. However, the thermal

treatment in high temperature (>750°C) usually worsens the dye loading ability. Therefore, there is a trade-off between the annealing temperature, the dye loading, and the PCE of DSSCs. So et al[19] reported that both increasing the annealing temperature from 450°C to 650°C and changing the annealing atmosphere from air to oxygen improved the PCE of TNT-based DSSCs due to the formation of a crystalline anatase structure.

4.7 | Other modifications

Yun et al[16] exposed the DSSCs to a light soaking in simulated sunlight (100 mW/cm^2, AM1.5G spectrum) for 5-60 minutes and obtained the highest efficiency enhancement of 168% on TNT15 sample (anodization time was 15 hours, tube length was 22 μm). The use of hydrochloric acid (HCl) to introduce hydroxyl groups on the surface of TNTs improved the dye loading from 137.8 nmol/cm^2 (untreated TNTs) to 230.0 nmol/cm^2 (0.1 mol/L HCl-treated TNTs).[116] The effect of the Ti metal substrate surface roughness on the PCE of TNT-based DSSCs has also been investigated. Combining mechanical polishing by sandpaper and electropolishing to give a very smooth Ti surface, yielded a higher TNT-DSSC PCE (1.61%) than that where the TNTs were grown on a rough substrate (0.72%).[117]

5 | SCALE EFFECTS AND STABILITY OF TNT-BASED DSSCs

For industrialization of DSSCs, large-area modules will be necessary.[118] However, typically the DSSC PCE decreases with increasing cell size.[13] TNT photoelectrodes on the other hand often ease the area dependent deterioration of the DSSC performance because of the good electron transporting abilities of the TNTs.[13]

Table 1[13,71] shows that increasing the cell size decreases the PCE in both TiO_2 NP-based and TNT-based DSSCs. When the cell size was 25 mm^2, the PCE of the TiO_2 NP-based and TNT-based DSSCs were 7.92% and 4.82%, respectively. When the cell size was increased to 900 mm^2, the PCE of the TiO_2 NP-based and TNT-based DSSCs decreased to 1.18% and 2.92%, respectively. The drop was clearly less with the TNT structure, which implies that the TNT-based DSSCs could have a potential for large-area application.

The highest PCE achieved with TNT-based DSSCs is over 10%.[19,31] However, for commercial applications of TNT-based DSSCs, long-term stability is another important factor. Unfortunately, the data available on this topic are very limited: only two studies related to the long-term stability of TNT-based DSSCs were found. Seidalilir et al[119] tested the stability TNT-based DSSCs with a liquid electrolyte and a polymer-based gel electrolyte containing poly (methyl methacrylate-*co*-ethyl acrylate) (7 wt.%) at 1 Sun illumination intensity and at 50°C for 1000 hours. The cells with liquid electrolyte degraded significantly after light soaking for 500 hours. The cell with the gel electrolyte retained 90% of the PCE after 1000 hours of light soaking. Hou et al[110] reported the PCE and degradation rates of TNT-based DSSCs placed in air for 0, 1, 2, 7, and 14 days. They showed that the PCE of the best performing cell with (initial PCE of 5.01%) decreased by 17.4% after 14 days light soaking under 100 mW/cm^2 (AM 1.5G).

6 | CONCLUSIONS

TiO_2 nanotubes are promising as photoelectrode material for dye-sensitized solar cells. Here, we have reviewed relevant literature on TNT-based DSSCs. The review identified three main methods to prepare TNTs for DSSCs: the anodic oxidation, the hydro/solvothermal, and the template method. The anodic oxidation method is the most used one, as it is simple and conformally controllable fabrication method yielding highly ordered nanotubes perpendicular to the substrate having a high length-to-diameter ratio.

The PCE of TNT-based DSSCs can be improved by modifying the TNTs through several ways, such as controlling the reaction time to adjust the geometry of the TNT in the preparation process, depositing metal oxide nanoparticles on the TNTs, $TiCl_4$ treatment, doping the TNTs, creating open the end of the tubes, and using different annealing conditions. Also, the relationship of the DSSC active area and the PCE was discussed. By increasing the cell size, the PCE of the DSSCs typically decreases, but for TNT-based DSSCs this is less dramatic than for the TiO_2 NP-based DSSCs.

It can be concluded that good electron transport and the possibility of large-area use are important positive attributes to the TNT-based DSSCs. However, the PCE of DSSCs still needs to be improved for commercial applications.[120] The highest efficiency of TNT-based DSSCs is presently 10.2%.[19] For the fabrication of TNT-based DSSCs, mostly N719 dye, thermally coated or sputtered Pt counter electrode and I_3^-/I^- redox mediator-based electrolyte are often used. A more systematic research of TNT-based DSSCs using different modification methods, dyes, electrolytes, and even other counter electrode structures/materials would be useful in order to find ways to improve the PCE. In addition to improving the efficiency, the question of the long-term stability of TNT-based DSSCs will need more scientific efforts in the future, as currently very little research on their stability is reported. It is also important to reduce the manufacturing costs of TNT-based DSSCs, by, for example, using cheaper materials.[121-126]

ACKNOWLEDGMENTS

This work has been supported by the China Scholarship Council (CSC), No. 201706250038, the Academy of Finland Flagship Programme, Photonics Research and Innovation (PREIN), No. 320167, and the Jane and Aatos Erkko Foundation ASPIRE project (Finland).

ORCID

Xuelan Hou https://orcid.org/0000-0001-9546-2643

REFERENCES

1. Shakeel Ahmad M, Pandey AK, Abd Rahim N. Advancements in the development of TiO_2 photoanodes and its fabrication methods for dye sensitized solar cell (DSSC) applications. A review. *Renew Sustain Energy Rev*. 2017;77:89-108.
2. So S, Hwang I, Schmuki P. Hierarchical DSSC structures based on "single walled" TiO_2 nanotube arrays reach a back-side illumination solar light conversion efficiency of 8%. *Energy Environ Sci*. 2015;8(3):849-854.
3. Aijo John K, Naduvath J, Remillard SK, et al. A simple method to fabricate metal doped TiO_2 nanotubes. *Chem Phys*. 2019;523:198-204.
4. Xie K, Guo M, Liu X, Huang H. Enhanced efficiencies in thin and semi-transparent dye-sensitized solar cells under low photon flux conditions using TiO_2 nanotube photonic crystal. *J Power Sources*. 2015;293:170-177.
5. Kakiage K, Aoyama Y, Yano T, Oya K, Fujisawa J, Hanaya M. Highly-efficient dye-sensitized solar cells with collaborative sensitization by silyl-anchor and carboxy-anchor dyes. *Chem Commun (Camb)*. 2015;51(88):15894-15897.
6. Halme J, Vahermaa P, Miettunen K, Lund P. Device physics of dye solar cells. *Adv Mater*. 2010;22(35):E210-E234.
7. Tsvetkov N, Larina L, Ku Kang J, Shevaleevskiy O. Sol-gel processed TiO_2 nanotube photoelectrodes for dye-sensitized solar cells with enhanced photovoltaic performance. *Nanomaterials (Basel)*. 2020;10(2), 296.
8. O'regan BAGM. A low-cost, high-efficiency solar cell based on dye-sensitized colloidal TiO_2 films. *Nature*. 1991;353(6346):737-740.
9. Zhou X, Nguyen NT, Özkan S, Schmuki P. Anodic TiO_2 nanotube layers: why does self-organized growth occur—a mini review. *Electrochem Commun*. 2014;46:157-162.
10. Wu WQ, Lei BX, Rao HS, et al. Hydrothermal fabrication of hierarchically anatase TiO_2 nanowire arrays on FTO glass for dye-sensitized solar cells. *Sci Rep*. 2013;3:1352.
11. Maçaira J, Andrade L, Mendes A. Review on nanostructured photoelectrodes for next generation dye-sensitized solar cells. *Renew Sustain Energy Rev*. 2013;27:334-349.
12. Lei BX, Liao JY, Zhang R, Wang J, Su CY, Kuang DB. Ordered crystalline TiO_2 nanotube arrays on transparent FTO glass for efficient dye-sensitized solar cells. *J Phys Chem C*. 2010;114(35):15228-15233.
13. Zhang Y, Khamwannah J, Kim H, Noh SY, Yang H, Jin S. Improved dye sensitized solar cell performance in larger cell size by using TiO_2 nanotubes. *Nanotechnology*. 2013;24(4):045401.
14. Roy P, Berger S, Schmuki P. TiO_2 nanotubes: synthesis and applications. *Angew Chem Int Ed Engl*. 2011;50(13):2904-2939.
15. Albu SP, Ghicov A, Macak JM, Schmuki P. 250 μm long anodic TiO_2 nanotubes with hexagonal self-ordering. *Phys Status Solidi Rapid Res Lett*. 2007;1(2):R65-R67.
16. Yun J-H, Mozer AJ, Wagner P, Offier DL, Amal R, Ng YH. Light soaking effect driven in porphyrin dye-sensitized solar cells using 1D TiO_2 nanotube photoanodes. *Sustain Mater Technol*. 2020;24:e00165.
17. Uchida S, Chiba R, Tomiha M, Masaki N, Shirai M. Application of titania nanotubes to a dye-sensitized solar cell. *Electrochem Commun*. 2002;70(6):418-420.
18. Macák JM, Tsuchiya H, Ghicov A, Schmuki P. Dye-sensitized anodic TiO_2 nanotubes. *Electrochem Commun*. 2005;7(11):1133-1137.
19. So S, Hwang I, Yoo J, et al. Inducing a nanotwinned grain structure within the TiO_2 nanotubes provides enhanced electron transport and DSSC efficiencies >10%. *Adv Energy Mater*. 2018;8(33):1800981.
20. Roy P, Kim D, Lee K, Spiecker E, Schmuki P. TiO_2 nanotubes and their application in dye-sensitized solar cells. *Nanoscale*. 2010;2(1):45-59.
21. Rho W-Y, Jeon H, Kim H-S, Chung W-J, Suh JS, Jun B-H. Recent progress in dye-sensitized solar cells for improving efficiency: TiO_2 nanotube arrays in active layer. *J Nanomater*. 2015;2015:1-17.
22. Gong J, Liang J, Sumathy K. Review on dye-sensitized solar cells (DSSCs): fundamental concepts and novel materials. *Renew Sustain Energy Rev*. 2012;16(8):5848-5860.
23. Yi Z, Zeng Y, Wu H, et al. Synthesis, surface properties, crystal structure and dye-sensitized solar cell performance of TiO_2 nanotube arrays anodized under different parameters. *Results Phys*. 2019;15:102609.
24. Luo D, Liu B, Fujishima A, Nakata K. TiO_2 nanotube arrays formed on Ti meshes with periodically arranged holes for flexible dye-sensitized solar cells. *ACS Appl Nano Mater*. 2019;2(6):3943-3950.
25. Ji Y, Zhang M, Cui J, et al. Highly-ordered TiO_2 nanotube arrays with double-walled and bamboo-type structures in dye-sensitized solar cells. *Nano Energy*. 2012;1(6):796-804.
26. Hou X, Jiang S, Li Y. A two-anode reduction technique to monitor the defect and dope the surface of TiO_2 nanotube array as photo-anode for water splitting. *Appl Catal B*. 2019;258:117949.
27. Gong D, Grimes CA, Varghese OK, et al. Titanium oxide nanotube arrays prepared by anodic oxidation. *J Mater Res*. 2001;16(12):3331-3334.
28. Macak JM, Tsuchiya H, Schmuki P. High-aspect-ratio TiO_2 nanotubes by anodization of titanium. *Angew Chem Int Ed Engl*. 2005;44(14):2100-2102.
29. Macak JM, Tsuchiya H, Taveira L, Aldabergerova S, Schmuki P. Smooth anodic TiO_2 nanotubes. *Angew Chem Int Ed Engl*. 2005;44(45):7463-7465.
30. Zhang G, Huang H, Zhang Y, Chan H, Zhou L. Highly ordered nanoporous TiO_2 and its photocatalytic properties. *Electrochem Commun*. 2007;9(12):2854-2858.
31. Qadir MB, Li Y, Sahito IA, et al. Highly functional TNTs with superb photocatalytic, optical, and electronic performance achieving record PV efficiency of 10.1% for 1D-based DSSCs. *Small*. 2016;12(33):4508-4520.
32. Chen H, Li N, Wu Y-H, Shi J-B, Lei B-X, Sun Z-F. A novel cheap, one-step and facile synthesis of hierarchical TiO_2 nanotubes as

fast electron transport channels for highly efficient dye-sensitized solar cells. *Adv Powder Technol*. 2020;31(4):1556–1563.
33. Chai Z, Gu J, Qiang P, Yu X, Mai W. Facile conversion of rutile titanium dioxide nanowires to nanotubes for enhancing the performance of dye-sensitized solar cells. *CrystEngComm*. 2015;17(5):1115-1120.
34. Xiao Y, Wu J, Yue G, Xie G, Lin J, Huang M. The preparation of titania nanotubes and its application in flexible dye-sensitized solar cells. *Electrochim Acta*. 2010;55(15):4573-4578.
35. Ri JH, Ryu GI, Ko SG, Kim B, Sonu KS. Anatase TiO_2 nanotubes-aggregated porous microspheres for Ti foil-based quasi-solid state dye-sensitized solar cells with improved photovoltaic performance. *J Electron Mater*. 2019;48(6):3459-3467.
36. Madurai Ramakrishnan V, Muthukumarasamy N, Balraju P, Pitchaiya S, Velauthapillai D, Pugazhendhi A. Transformation of TiO_2 nanoparticles to nanotubes by simple solvothermal route and its performance as dye-sensitized solar cell (DSSC) photoanode. *Int J Hydrogen Energy*. 2020;45(31):15441-15452.
37. Liu Y-Y, Ye X-Y, Chen H, et al. Self-templated synthesis of large-scale hierarchical anatase titania nanotube arrays on transparent conductive substrate for dye-sensitized solar cells. *Adv Powder Technol*. 2019;30(3):572-580.
38. Hashmi G, Miettunen K, Peltola T, et al. Review of materials and manufacturing options for large area flexible dye solar cells. *Renew Sustain Energy Rev*. 2011;15(8):3717-3732.
39. Miettunen K, Halme J, Lund P. Metallic and plastic dye solar cells. *Wiley Interdiscip Rev Energy Environ*. 2013;2(1):104-120.
40. Huang CH, Chen YW, Chen CM. Chromatic titanium photoanode for dye-sensitized solar cells under rear illumination. *ACS Appl Mater Interfaces*. 2018;10(3):2658-2666.
41. Rui Y, Wang Y, Zhang Q, et al. In-situ construction of three-dimensional titania network on Ti foil toward enhanced performance of flexible dye-sensitized solar cells. *Appl Surf Sci*. 2016;380:210-217.
42. Kowalski D, Kim D, Schmuki P. TiO_2 nanotubes, nanochannels and mesosponge: self-organized formation and applications. *Nano Today*. 2013;8(3):235-264.
43. Fu N, Li X, Liu Y, et al. Low temperature transfer of well-tailored TiO_2 nanotube array membrane for efficient plastic dye-sensitized solar cells. *J Power Sources*. 2017;343:47-53.
44. Zhu W, Liu Y, Yi A, Zhu M, Li W, Fu N. Facile fabrication of open-ended TiO_2 nanotube arrays with large area for efficient dye-sensitized solar cells. *Electrochim Acta*. 2019;299:339-345.
45. Liang J, Yang J, Zhang G, Sun W. Flexible fiber-type dye-sensitized solar cells based on highly ordered TiO_2 nanotube arrays. *Electrochem Commun*. 2013;37:80-83.
46. Song CB, Qiang YH, Zhao YL, et al. Dye-sensitized solar cells based on graphene-TiO_2 nanoparticles/TiO_2 nanotubes composite films. *Int J Electrochem Sci*. 2014;9:8090-8096.
47. Zhao YL, Song DM, Qiang YH, Gu XQ, Zhu L, Song CB. Dye-sensitized solar cells based on TiO_2 hollow spheres/TiO_2 nanotube array composite films. *Appl Surf Sci*. 2014;309:85-89.
48. Zheng Q, Kang H, Yun J, Lee J, Park JH, Baik S. Hierarchical construction of self-standing anodized titania nanotube arrays and nanoparticles for efficient and cost-effective front-illuminated dye-sensitized solar cells. *ACS Nano*. 2011;5(6):5088-5093.
49. Pang Q, Leng L, Zhao L, Zhou L, Liang C, Lan Y. Dye sensitized solar cells using freestanding TiO_2 nanotube arrays on FTO substrate as photoanode. *Mater Chem Phys*. 2011;125(3):612-616.
50. Song CB, Qiang YH, Zhao YL, Gu XQ, Song DM, Zhu L. Adhesion of TiO_2 nanotube arrays on transparent conducting substrates using CNT–TiO_2 composite pastes. *Appl Surf Sci*. 2014;305:792-796.
51. Paulose M, Shankar K, Varghese OK, Mor GK, Hardin B, Grimes CA. Backside illuminated dye-sensitized solar cells based on titania nanotube array electrodes. *Nanotechnology*. 2006;17(5):1446-1448.
52. Chun KY, Park BW, Sung YM, Kwak DJ, Hyun YT, Park MW. Fabrication of dye-sensitized solar cells using TiO_2-nanotube arrays on Ti-grid substrates. *Thin Solid Films*. 2009;517(14):4196-4198.
53. Liu N, Chen X, Zhang J, Schwank JW. A review on TiO_2-based nanotubes synthesized via hydrothermal method: formation mechanism, structure modification, and photocatalytic applications. *Catal Today*. 2014;225:34-51.
54. Kim Y-G, Shim C-H, Kim D-H, Lee HJ, Lee H-J. Fabrication of transparent conductive oxide-less dye-sensitized solar cells consisting of Ti electrodes by electron-beam evaporation process. *Thin Solid Films*. 2012;520(6):2257-2260.
55. Ghanavatinejad M, Ghorashi SMB, Chamanzadeh Z. Preparation and characterization of vertical regular arrayed and needle-shaped irregular titanium dioxide nanotubes for dye-sensitized solar cells. *Optik*. 2020;203:163432.
56. Kathirvel S, Su C, Yang C-Y, Shiao Y-J, Chen B-R, Li W-R. The growth of TiO_2 nanotubes from sputter-deposited Ti film on transparent conducting glass for photovoltaic applications. *Vacuum*. 2015;118:17-25.
57. Krumpmann A, Dervaux J, Derue L, et al. Influence of a sputtered compact TiO_2 layer on the properties of TiO_2 nanotube photoanodes for solid-state DSSCs. *Mater Des*. 2017;120:298-306.
58. Nguyen HH, Gyawali G, Martinez-Oviedo A, Kshetri YK, Lee SW. Physicochemical properties of Cr-doped TiO_2 nanotubes and their application in dye-sensitized solar cells. *J Photochem Photobiol A*. 2020;397:112514.
59. Lee K-M, Suryanarayanan V, Huang J-H, Thomas KRJ, Lin JT, Ho K-C. Enhancing the performance of dye-sensitized solar cells based on an organic dye by incorporating TiO_2 nanotube in a TiO_2 nanoparticle film. *Electrochim Acta*. 2009;54(16):4123-4130.
60. Yen Y-C, Ko W-Y, Chen J-Z, Lin K-J. Enhancing the performance of dye-sensitized solar cells based on TiO_2 nanotube/nanoparticle composite photoanodes. *Electrochim Acta*. 2013;105:142-148.
61. Karimipour M, Mashhoun S, Mollaei M, Molaei M, Taghavinia N. A simple low pressure method for the synthesis of TiO_2 nanotubes and nanofibers and their application in DSSCs. *Electron Mater Lett*. 2015;11(4):625-632.
62. Hao NH, Gyawali G, Sekino T, Lee SW. Fabrication of a TiO_2-P25/(TiO_2-P25+TiO_2 nanotubes) junction for dye sensitized solar cells. *Prog Nat Sci Mater Int*. 2016;26(4):375-379.
63. Roh DK, Chi WS, Jeon H, Kim SJ, Kim JH. High efficiency solid-state dye-sensitized solar cells assembled with hierarchical anatase pine tree-like TiO_2 nanotubes. *Adv Func Mater*. 2014;24(3):379-386.
64. Zhuge F, Qiu J, Li X, Gao X, Gan X, Yu W. Toward hierarchical TiO_2 nanotube arrays for efficient dye-sensitized solar cells. *Adv Mater*. 2011;23(11):1330-1334.
65. Zhang J, Kusumawati Y, Pauporté T. Dye-sensitized solar cells based on TiO_2 nanotube and shelled arrayed structures. *Electrochim Acta*. 2016;201:125-133.

66. Xu C, Gao D. Two-stage hydrothermal growth of long ZnO nanowires for efficient TiO_2 nanotube-based dye-sensitized solar cells. *J Phys Chem C*. 2012;116(12):7236-7241.
67. Lee J, Hong KS, Shin K, Jho JY. Fabrication of dye-sensitized solar cells using ordered and vertically oriented TiO_2 nanotube arrays with open and closed ends. *J Ind Eng Chem*. 2012;18(1):19-23.
68. Tian H, Chen K, Ye X, Yang S, Gu Q. Hydrothermal growth of $Bi_2Ti_2O_7/TiO_2$ and $Bi_4Ti_3O_{12}/TiO_2$ heterostructures on highly ordered TiO_2-nanotube arrays for dye-sensitized solar cells. *Ceram Int*. 2019;45(16):20750-20757.
69. Liu Z, Misra M. Dye-sensitized photovoltaic wires using highly ordered TiO_2 nanotube arrays. *ACS Nano*. 2010;4(4):2196-2200.
70. Wu TL, Meen TH, Ji LW, et al. Fabrication of open-end TiO_2 nanotubes attached to front-illuminated dye-sensitized solar cells. *Sensors Mater*. 2016;28(5):539-545.
71. Zhang J, Li S, Ding H, et al. Transfer and assembly of large area TiO_2 nanotube arrays onto conductive glass for dye sensitized solar cells. *J Power Sources*. 2014;247:807-812.
72. Paulose M, Shankar K, Varghese OK, Mor GK, Grimes CA. Application of highly-ordered TiO_2 nanotube-arrays in heterojunction dye-sensitized solar cells. *J Phys D Appl Phys*. 2006;39(12):2498-2503.
73. Varghese OK, Paulose M, Grimes CA. Long vertically aligned titania nanotubes on transparent conducting oxide for highly efficient solar cells. *Nat Nanotechnol*. 2009;4(9):592-597.
74. Li S, Liu Y, Zhang G, Zhao X, Yin J. The role of the TiO_2 nanotube array morphologies in the dye-sensitized solar cells. *Thin Solid Films*. 2011;520(2):689-693.
75. Lin J, Liu K, Chen X. Synthesis of periodically structured titania nanotube films and their potential for photonic applications. *Small*. 2011;7(13):1784-1789.
76. Yip CT, Huang H, Zhou L, et al. Direct and seamless coupling of TiO_2 nanotube photonic crystal to dye-sensitized solar cell: a single-step approach. *Adv Mater*. 2011;23(47):5624-5628.
77. Joseph S, Melvin Boby SJ, Theresa Nathan DMG, Sagayaraj P. Investigation on the role of cost effective cathode materials for fabrication of efficient DSSCs with $TiNT/TiO_2$ nanocomposite photoanodes. *Sol Energy Mater Sol Cells*. 2017;165:72-81.
78. Nyein N, Tan WK, Kawamura G, Matsuda A, Lockman Z. TiO_2 nanotube arrays formation in fluoride/ethylene glycol electrolyte containing LiOH or KOH as photoanode for dye-sensitized solar cell. *J Photochem Photobiol A*. 2017;343:33-39.
79. Guo M, Chen J, Zhang J, et al. Coupling plasmonic nanoparticles with TiO_2 nanotube photonic crystals for enhanced dye-sensitized solar cells performance. *Electrochim Acta*. 2018;263:373-381.
80. Guo M, Xie K, Lin J, et al. Design and coupling of multifunctional TiO_2 nanotube photonic crystal to nanocrystalline titania layer as semi-transparent photoanode for dye-sensitized solar cell. *Energy Environ Sci*. 2012;5(12):9881.
81. Ghani T, Mujahid M, Mehmood M, Zhang G, Naz S. Highly ordered combined structure of anodic TiO_2 nanotubes and TiO_2 nanoparticles prepared by a novel route for dye-sensitized solar cells. *J Saudi Chem Soc*. 2019;23(8):1231-1240.
82. Tien MS, Lin LY, Xiao BC, Hong ST. Enhancing the contact area of Ti wire as photoanode substrate of flexible fiber-type dye-sensitized solar cells using the TiO_2 nanotube growth and removal technique. *Nanomaterials (Basel)*. 2019;9(11):1521.
83. Rho W-Y, Kim H-S, Chung W-J, Suh JS, Jun B-H, Hahn Y-B. Enhancement of power conversion efficiency with TiO_2 nanoparticles/nanotubes-silver nanoparticles composites in dye-sensitized solar cells. *Appl Surf Sci*. 2018;429:23-28.
84. Rho C, Suh JS. Filling TiO_2 nanoparticles in the channels of TiO_2 nanotube membranes to enhance the efficiency of dye-sensitized solar cells. *Chem Phys Lett*. 2011;513(1-3):108-111.
85. Zhang J, Li Q, Li S, et al. An efficient photoanode consisting of TiO_2 nanoparticle-filled TiO_2 nanotube arrays for dye sensitized solar cells. *J Power Sources*. 2014;268:941-949.
86. Fu N, Jiang X, Chen D, et al. Au/TiO_2 nanotube array based multi-hierarchical architecture for highly efficient dye-sensitized solar cells. *J Power Sources*. 2019;439:227076.
87. Rho WY, Chun MH, Kim HS, Kim HM, Suh JS, Jun BH. Ag nanoparticle-functionalized open-ended freestanding TiO_2 nanotube arrays with a scattering layer for improved energy conversion efficiency in dye-sensitized solar cells. *Nanomaterials (Basel)*. 2016;6(6):117.
88. Lee JS, Kim KH, Kim CS, Choi HW. Achieving enhanced dye-sensitized solar cell performance by $TiCl_4/Al_2O_3$ doped TiO_2 nanotube array photoelectrodes. *J Nanomater*. 2015;2015:1-6.
89. Elzarka A, Liu N, Hwang I, Kamal M, Schmuki P. Large-diameter TiO_2 nanotubes enable wall engineering with conformal hierarchical decoration and blocking layers for enhanced efficiency in dye-sensitized solar cells (DSSC). *Chemistry*. 2017;23(53):12995-12999.
90. Chamanzadeh Z, Noormohammadi M, Zahedifar M. Enhanced photovoltaic performance of dye sensitized solar cell using TiO_2 and ZnO nanoparticles on top of free standing TiO_2 nanotube arrays. *Mater Sci Semicond Process*. 2017;61:107-113.
91. Kim J-Y, Shin K-Y, Raza MH, Pinna N, Sung Y-E. Vertically aligned TiO_2/ZnO nanotube arrays prepared by atomic layer deposition for photovoltaic applications. *Korean J Chem Eng*. 2019;36(7):1157-1163.
92. Bozkurt Çırak B, Eden Ç, Erdoğan Y, et al. The enhanced light harvesting performance of dye-sensitized solar cells based on ZnO nanorod-TiO_2 nanotube hybrid photoanodes. *Optik*. 2020;203:163963.
93. So S, Kriesch A, Peschel U, Schmuki P. Conical-shaped titania nanotubes for optimized light management in DSSCs reach back-side illumination efficiencies > 8%. *J Mater Chem A*. 2015;3(24):12603-12608.
94. Ye M, Xin X, Lin C, Lin Z. High efficiency dye-sensitized solar cells based on hierarchically structured nanotubes. *Nano Lett*. 2011;11(8):3214-3220.
95. Park J-H, Kim J-Y, Kim J-H, et al. Enhanced efficiency of dye-sensitized solar cells through $TiCl_4$-treated, nanoporous-layer-covered TiO_2 nanotube arrays. *J Power Sources*. 2011;196(20):8904-8908.
96. Rezaei B, Mohammadi I, Ensafi AA, Momeni MM. Enhanced efficiency of DSSC through AC-electrophoretic hybridization of TiO_2 nanoparticle and nanotube. *Electrochim Acta*. 2017;247:410-419.
97. Yang D-J, Park H, Cho S-J, Kim H-G, Choi W-Y. TiO_2-nanotube-based dye-sensitized solar cells fabricated by an efficient anodic oxidation for high surface area. *J Phys Chem Solids*. 2008;69(5-6):1272-1275.
98. Lee K, Schmuki P. Ta doping for an enhanced efficiency of TiO_2 nanotube based dye-sensitized solar cells. *Electrochem Commun*. 2012;25:11-14.
99. Rho WY, Lee KH, Han SH, Kim HY, Jun BH. Au-embedded and carbon-doped freestanding TiO_2 nanotube arrays in dye-sensitized solar cells for better energy conversion efficiency. *Micromachines (Basel)*. 2019;10(12):805.

100. Peighambardoust NS, Asl SK, Mohammadpour R, Asl SK. Improved efficiency in front-side illuminated dye sensitized solar cells based on free-standing one-dimensional TiO_2 nanotube array electrodes. *Sol Energy*. 2019;184:115-126.
101. Ohsaki Y, Masaki N, Kitamura T, et al. Dye-sensitized TiO_2 nanotube solar cells: fabrication and electronic characterization. *Phys Chem Chem Phys*. 2005;7(24):4157-4163.
102. Yang H-Y, Lee SH, Kim H-M, et al. Plasmonic and charging effects in dye-sensitized solar cells with Au nanoparticles incorporated into the channels of freestanding TiO_2 nanotube arrays by an electrodeposition method. *J Ind Eng Chem*. 2019;80:311-317.
103. Wang Z, Tang Y, Li M, et al. Plasmonic enhancement of the performance of dye-sensitized solar cells by incorporating TiO_2 nanotubes decorated with Au nanoparticles. *J Alloy Compd*. 2017;714:89-95.
104. Hu J, Cheng J, Tong S, Yang Y, Chen M, Hu S. Ag-doped TiO_2 nanotube arrays composite film as a photoanode for enhancing the photoelectric conversion efficiency in DSSCs. *Int J Photoenergy*. 2016;2016:1-9.
105. Wei X, Nbelayim PS, Kawamura G, Muto H, Matsuda A. Ag nanoparticle-filled TiO_2 nanotube arrays prepared by anodization and electrophoretic deposition for dye-sensitized solar cells. *Nanotechnology*. 2017;28(13):135207.
106. Rho W-Y, Kim H-S, Lee SH, et al. Front-illuminated dye-sensitized solar cells with Ag nanoparticle-functionalized freestanding TiO_2 nanotube arrays. *Chem Phys Lett*. 2014;614:78-81.
107. Liu C, Li T, Zhang Y, et al. Silver nanoparticle modified TiO_2 nanotubes with enhanced the efficiency of dye-sensitized solar cells. *Microporous Mesoporous Mater*. 2019;287:228-233.
108. Luan X, Chen L, Zhang J, Qu G, Flake JC, Wang Y. Electrophoretic deposition of reduced graphene oxide nanosheets on TiO_2 nanotube arrays for dye-sensitized solar cells. *Electrochim Acta*. 2013;111:216-222.
109. Wang S, Zhang J, Chen S, et al. Conversion enhancement of flexible dye-sensitized solar cells based on TiO_2 nanotube arrays with TiO_2 nanoparticles by electrophoretic deposition. *Electrochim Acta*. 2011;56(17):6184-6188.
110. Hou Z, Que W, Ren J, et al. Fabrication and stability of opened-end TiO_2 nanotube arrays based dye-sensitized solar cells. *Ceram Int*. 2015;41:S719-S724.
111. Hossain MA, Oh S, Lim S. Fabrication of dye-sensitized solar cells using a both-ends-opened TiO_2 nanotube/nanoparticle hetero-nanostructure. *J Ind Eng Chem*. 2017;51:122-128.
112. Lin C-J, Yu W-Y, Chien S-H. Transparent electrodes of ordered opened-end TiO_2-nanotube arrays for highly efficient dye-sensitized solar cells. *J Mater Chem*. 2010;20(6):1073-1077.
113. Mohammadpour F, Altomare M, So S, et al. High-temperature annealing of TiO_2 nanotube membranes for efficient dye-sensitized solar cells. *Semicond Sci Technol*. 2016;31(1):014010.
114. Jeyaraman AR, Balasingam SK, Lee C, et al. Enhanced solar to electrical energy conversion of titania nanoparticles and nanotubes-based combined photoanodes for dye-sensitized solar cells. *Mater Lett*. 2019;243:180-182.
115. Lin J, Guo M, Yip CT, et al. High temperature crystallization of free-standing anatase TiO_2 nanotube membranes for high efficiency dye-sensitized solar cells. *Adv Func Mater*. 2013;23(47):5952-5960.
116. Liu T, Wang B, Xie J, et al. Photovoltaic properties of dye sensitised solar cells using TiO_2 nanotube arrays for photoanodes: role of hydrochloric acid treatment. *Appl Surf Sci*. 2015;355:256-261.
117. Pourandarjani A, Nasirpouri F. Tuning substrate roughness to improve uniform growth and photocurrent response in anodic TiO_2 nanotube arrays. *Ceram Int*. 2018;44(18):22671-22679.
118. Bella F, Lamberti A, Sacco A, Bianco S, Chiodoni A, Bongiovanni R. Novel electrode and electrolyte membranes: towards flexible dye-sensitized solar cell combining vertically aligned TiO_2 nanotube array and light-cured polymer network. *J Membr Sci*. 2014;470:125-131.
119. Seidalilir Z, Malekfar R, Wu HP, Shiu JW, Diau EW. High-performance and stable gel-state dye-sensitized solar cells using anodic TiO_2 nanotube arrays and polymer-based gel electrolytes. *ACS Appl Mater Interfaces*. 2015;7(23):12731-12739.
120. Gong J, Sumathy K, Qiao Q, Zhou Z. Review on dye-sensitized solar cells (DSSCs): advanced techniques and research trends. *Renew Sustain Energy Rev*. 2017;68:234-246.
121. Jo Y, Cheon JY, Yu J, et al. Highly interconnected ordered mesoporous carbon-carbon nanotube nanocomposites: Pt-free, highly efficient, and durable counter electrodes for dye-sensitized solar cells. *Chem Commun (Camb)*. 2012;48(65):8057-8059.
122. Yan J, Uddin MJ, Dickens TJ, Okoli OI. Carbon nanotubes (CNTs) enrich the solar cells. *Sol Energy*. 2013;96:239-252.
123. Zhang C, Xie Y, Ma J, Hu J, Zhang C. A composite catalyst of reduced black TiO_{2-x}/CNT: a highly efficient counter electrode for ZnO-based dye-sensitized solar cells. *Chem Commun (Camb)*. 2015;51(98):17459-17462.
124. Wongcharee K, Meeyoo V, Chavadej S. Dye-sensitized solar cell using natural dyes extracted from rosella and blue pea flowers. *Sol Energy Mater Sol Cells*. 2007;91(7):566-571.
125. Li N, Pan N, Li D, Lin S. Natural dye-sensitized solar cells based on highly ordered TiO_2 nanotube arrays. *Int J Photoenergy*. 2013;2013:1-5.
126. Sathyajothi S, Jayavel R, Dhanemozhi AC. The fabrication of natural dye sensitized solar cell (Dssc) based on TiO_2 using henna and beetroot dye extracts. *Mater Today Proc*. 2017;4(2):668-676.

How to cite this article: Hou X, Aitola K, Lund PD. TiO_2 nanotubes for dye-sensitized solar cells—A review. *Energy Sci Eng*. 2020;00:1–17. https://doi.org/10.1002/ese3.831